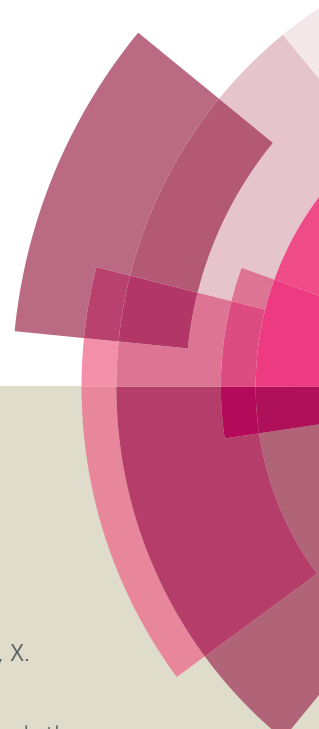


Journal of Materials Chemistry B

Accepted Manuscript



This article can be cited before page numbers have been issued, to do this please use: L. Chen, X. Yao, X. Chen, C. He and X. Chen, *J. Mater. Chem. B*, 2015, DOI: 10.1039/C5TB00256G.



This is an *Accepted Manuscript*, which has been through the Royal Society of Chemistry peer review process and has been accepted for publication.

Accepted Manuscripts are published online shortly after acceptance, before technical editing, formatting and proof reading. Using this free service, authors can make their results available to the community, in citable form, before we publish the edited article. We will replace this *Accepted Manuscript* with the edited and formatted *Advance Article* as soon as it is available.

You can find more information about *Accepted Manuscripts* in the [Information for Authors](#).

Please note that technical editing may introduce minor changes to the text and/or graphics, which may alter content. The journal's standard [Terms & Conditions](#) and the [Ethical guidelines](#) still apply. In no event shall the Royal Society of Chemistry be held responsible for any errors or omissions in this *Accepted Manuscript* or any consequences arising from the use of any information it contains.

Cite this: DOI: 10.1039/c0xx00000x

www.rsc.org/xxxxxx

ARTICLE TYPE

Dual pH-Responsive Mesoporous Silica Nanoparticles for Efficient Combination of Chemotherapy and Photodynamic Therapy

Xuemei Yao^a, Xiaofei Chen^a, Chaoliang He^b, Li Chen^{a*}, Xuesi Chen^b

Received (in XXX, XXX) Xth XXXXXXXXX 20XX, Accepted Xth XXXXXXXXX 20XX

DOI: 10.1039/b000000x

A kind of dual pH-responsive mesoporous silica nanoparticles (MSNs)-based drug delivery system, which can respond to the cancer extracellular and intercellular pH stimuli, has been fabricated for synergistic chemo-photodynamic therapy. By grafting histidine onto the silica surface, the acid sensitive PEGylated tetraphenylporphyrin zinc (Zn-Por-CA-PEG) can be acted as gatekeeper to block the nanopores of MSNs by the metallo-supramolecular-coordinated interaction between Zn-Por and histidine. This gatekeeper is stable enough to prevent loaded-drug from leaching out at health tissue. However, at cancer extracellular pH (~6.8) the conjugated acid sensitive *cis*-aconitic anhydride (CA) between Zn-Por and PEG will cleave and the surface of Zn-Por will be amino positively charged to facilitate cell internalization. Furthermore, the metallo-surpmolecular-coordination will disassemble at intracellular acidic microenvironments (~5.3) to release the carried drug and Zn-Por due to the removal of gatekeeper. The photosensitivity of Zn-Por further make it possible to combine chemotherapy and photodynamic therapy. This dual pH-sensitive MSNs-based drug delivery system has showed higher *in vitro* cytotoxicity than the single chemotherapy of free DOX or photodynamic therapy of Zn-Por, presenting its great potential for cancer treatments to overcome the challenges of efficient delivery in site and ideal anti-cancer efficacy.

1 Introduction

Advancement in nanotechnology provides enormous opportunities to cancer therapeutics. With nontoxic nature, easily modifiable surface and good biocompatibility, uniform mesoporous silica nanoparticles (MSNs), as a leading kind of nanocontainer, have attracted tremendous interest.¹⁻³ Due to the controllable mesoporous structure, high specific surface area and large pore volume, MSNs present high drug loading capacity, smart drug release behavior, and co-delivery capability.⁴ Mesoporous silica sustained drug delivery systems, which can pack drug molecules into the channels of mesoporous silica materials by simple physical adsorption, will cause immediate drug release after administration.^{5, 6} To reduce the severe side-effect and enhance the anti-cancer efficacy, it is highly desirable to design stimuli-responsive controlled drug delivery systems, in which the caps can be closed in normal conditions and opened in demand. In this kind of system, the mesopores loaded with drug can be capped by various stimuli-responsive “gatekeepers”.

It is known that the biological microenvironment in cancer tissues is different from that in physiologically normal cells and tissues. Up to now, several sophisticated stimuli-responsive drug delivery systems based on MSNs have been described. In these systems, the efficient release of drug form MSNs are regulated by biological stimuli, such as redox,^{7, 8} pH,^{9, 10} temperature^{11, 12} and enzyme.^{13, 14} Among these stimuli, pH-triggered release is a particularly attractive option since certain tissues of the body, such as cancers and inflammatory tissues (pH ≈ 6.8), endosomal and lysosomal cell compartments (pH ≈ 5.5), have a more acidic pH than blood or healthy tissues (pH ≈ 7.4).¹⁵ These pH-sensitive human systems and tissues provide an efficient way to control the drug release behavior by pH-stimuli. Generally, supramolecular

nanovalves,¹⁶ proteins,¹⁷ polymers¹⁸ or nucleic acids¹⁹ are used as gatekeepers to fabricate pH-controlled MSN release systems. For example, Zhou had reported a kind of pH-responsive natural gelatin capped mesoporous silica nanoparticles (MSN@Gelatin) as intracellular drug delivery. The gelatin capping layer could effectively prohibit the release of loaded drug molecules in neutral pH environment. While the slightly acidic environment would enhance the electrostatic repulsion between the gelatin and MSN, giving rise to uncapping and the subsequent controlled release of the entrapped drug.²⁰ Che and co-workers had reported a novel coordination polymers (CPs)-coated MSN drug delivery, which capped by the CPs of zinc and 1,4-bis(imidazol-1-ylmethyl) benzene (BIX) grown on the MSNs surfaces, serving as a pH-responsive nanocarrier for efficient targeted drug delivery to cancer cells.²¹

In current clinical therapy, administering single drug or exploring single treatment is not successful as expected. A combination of multiple anticancer agents or different types of therapy has been widely explored to enhance clinical anticancer efficiency, such as the combination of chemotherapy with phototherapy²² or photothermal therapy.²³ Photodynamic therapy (PDT) is a type of phototherapy, which is based on the concept of photosensitizers. When photosensitizers were exposed to light of specific wavelength, the generated cytotoxic reactive oxygen species (ROS) is capable of killing cancer cells.^{24, 25} Metalloporphyrins, as a type of photosensitizer, have been widely used in clinical photodynamic therapy for the effective generation of ROS. However, most of porphyrins and their derivatives are hydrophobic. The lipophilic nature makes them undispersed and unstable in an aqueous medium, which greatly limits their applications *in vivo*.^{26, 27} To overcome these problems, the delivery systems for porphyrins or their derivatives such as liposomes, polymeric particles, hydrophilic polymer, or

with triethylamine as catalyst. For typical synthesis procedure of Zn-Por-CA, Zn-Por-NH₂ (100 mg, 0.14 mmol) and CA (84 mg, 0.54 mmol) were dissolved in 10.0 mL of anhydrous DMF in a dried flask, and then 74 μ L of anhydrous triethylamine was added. The mixture was stirred under a nitrogen environment at room temperature for 24 h. After that, the solution was mixed with 100.0 mL of cold ethyl acetate, and then the mixture was washed with cold acidic saturated sodium chloride solution (pH 2–3) and finally with normal saturated solution (pH 7.4). The organic layer was collected and dried with anhydrous sodium sulfate overnight. After filtration, the filtrate was dried under vacuum at room temperature to obtain product. Zn-Por-SA was synthesized with the same approach as Zn-Por-CA.

2.5 Synthesis of PEGylated Zn-Por-CA (Zn-Por-CA-PEG) and PEGylated Zn-Por-SA (Zn-Por-SA-PEG)

Zn-Por-CA-PEG and Zn-Por-SA-PEG were separately synthesized through the condensation reaction between PEG and Zn-Por-CA or Zn-Por-SA with EDC·HCl and DMAP as condensing agent and catalyst, respectively. For example, PEG (500 mg, 0.25 mmol) was dissolved in DMF, and then Zn-Por-CA (72 mg, 0.1 mmol), EDC·HCl (39 mg, 0.2 mmol), and DMAP (2.4 mg, 0.02 mmol) were added to the solution. The mixture was stirred at room temperature for 48 h. Then, Zn-Por-CA-PEG was obtained through a dialysis method (molecular weight cutoff (MWCO) = 3500 Da) against deionized water for 48 h. Zn-Por-SA-PEG was synthesized with the similar approach as Zn-Por-CA-PEG.

2.6 Synthesis of histidine modified mesoporous silica nanoparticles (MSN-His)

MSN-NH₂ was synthesized as our team previous works.³⁴ MSN-NH₂ (0.03 g) was dispersed in 70 mL of anhydrous DMSO, and then BOC-histidine (2.55 g, 0.01 mol), EDC·HCl (3.94 g, 0.02 mol) and NHS (2.76 g, 0.024 mol) were added into the solution. The reaction mixture was stirred at 25 °C for 48 h. After the reaction, the mixture was centrifuged (9500 rpm, 10 min), and washed twice with methanol and dried under vacuum overnight.

2.7 Synthesis of Zn-Por-CA-PEG or Zn-Por-SA-PEG capped MSNs (MSN-Por-CA-PEG or MSN-Por-SA-PEG)

MSN-His (0.03 g) and Zn-Por-CA-PEG (0.35 g) were dissolved in 10 mL of DMSO. The mixture was stirred at 25 °C for 72 h. Then, MSN-Por-CA-PEG was obtained by centrifugation (9500 rpm, 10 min), and washed six times with methanol and dried under vacuum overnight. MSN-Por-SA-PEG was got as similar way with MSN-Por-CA-PEG.

2.8 *In vitro* drug loading and release

Doxorubicin (DOX) was used as a model drug for *in vitro* drug loading and release. DOX loaded MSN-Por-CA-PEG were prepared by a simple dialysis technique. Typically, MSN-His (14.0 mg), Zn-Por-CA-PEG (117 mg) and drug (30 mg) were mixed in 10 mL of DMSO. The mixture was stirred at room temperature for 24 h and then added dropwise into 50.0 mL of PBS at pH 7.4. The DMSO was removed by dialysis against water at pH 7.4 for 24 h. The dialysis medium was refreshed four times and the whole procedure was performed in the dark. After removing the blank particles by centrifugation, the supernatant was measured by UV-Vis spectrophotometer. According to a standard curve obtained from DOX/DMSO solutions at a series of DOX concentrations, we obtained drug loading content. DOX-loaded MSN-Por-SA-PEG was got as similar way.

In vitro drug release profiles of drug-loaded MSNs were

investigated in PBS (pH 5.3, 6.8 or 7.4). The pre-weighed freeze-dried DOX loaded MSNs were suspended in 4 mL of release medium and transferred into a dialysis bag (MWCO 3500 Da). The release experiment was initiated by placing the end-sealed dialysis bag into 50 mL of release medium at 37 °C with continuous shaking at 70 rpm. At predetermined intervals, 2 mL of external release medium was taken out and an equal volume of fresh release medium was replenished. The amount of released DOX was determined by using fluorescence measurement. The release experiments were conducted in triplicate.

2.9 Intracellular drug release

The cellular uptake and intracellular release behaviors of DOX-loaded MSNs were assessed by confocal laser scanning microscopy (CLSM) and flow cytometric analyses on HeLa cells.

2.9.1 CLSM

For CLSM study, HeLa cells were seeded in 6-well plates at a density of 10⁵ cells per well in 2.0 mL of complete Dulbecco's modified Eagle's medium (DMEM) containing 10 % fetal bovine serum, supplemented with 50 IU mL⁻¹ penicillin and 50 IU mL⁻¹ streptomycin. After incubation for 24 h, the culture media were withdrawn and culture media containing MSN-Por-CA-PEG or MSN-Por-SA-PEG were supplemented (final Zn-Por concentration: 9 mg L⁻¹). The cells were incubated for another 2 h at 37 °C and 4 °C. After washed with PBS five times, the cells were then fixed in 4% paraformaldehyde for 20 min and washed with PBS five times. For staining the nuclei, the cells were incubated with 4',6-diamidino-2-phenylindole (DAPI, blue) for 2 min. The images of cells were observed using a laser scanning confocal microscope (Olympus FluoView 1000).

2.9.2 Flow cytometric analyses

HeLa cells were placed into 6-well plates (2 × 10⁵ cells/well) and cultured in 2.0 mL of complete DMEM for 24 h. The culture media were then withdrawn and culture media with MSN-Por-CA-PEG or MSN-Por-SA-PEG were supplemented at a final Zn-Por concentration of 9 mg L⁻¹. The cells were incubated for additional 2 h, followed by washing with PBS three times and trypsinized. Then, 1.0 mL of PBS was added, and the solutions were centrifuged for 4 min at 3000 rpm and the cells were resuspended in 0.3 mL of PBS. The analysis was performed by flow cytometer (Beckman, California, U.S.A.) for 1 × 10⁴ cells.

2.10 Cell viability assays

The relative cytotoxicities of MSN-Por-CA-PEG or MSN-Por-SA-PEG in the dark against HeLa and MCF-7 cells were evaluated *in vitro* by a standard MTT assay. The cells were seeded in 96-well plates at 1 × 10⁴ cells per well in 200.0 μ L of complete DMEM and incubated at 37 °C in 5 % CO₂ atmosphere for 24 h. The culture medium was then removed and MSN-Por-CA-PEG or MSN-Por-SA-PEG solutions in complete DMEM at different concentrations (0–10 g L⁻¹) were added. The cells were subjected to MTT assay after being incubated for additional 48 h. The absorbance of the solution was measured on a Bio-Rad 680 microplate reader at 490 nm. Cell viability (%) was calculated based on eqn (1):

$$\text{Cell viability (\%)} = A_{\text{sample}} / A_{\text{control}} \times 100 \quad (1)$$

where, A_{sample} and A_{control} represent the absorbances of the sample and control wells, respectively.

The cytotoxicities of DOX-loaded MSNs against HeLa and MCF-7 cells were also evaluated *in vitro* by a MTT assay. Similarly, cells were seeded into 96-well plates at 7 × 10³ cells

per well in 200.0 μL of complete DMEM and further incubated for 24 h. After washing cells with PBS, 180.0 μL of complete DMEM and 20.0 μL of DOX-loaded MSN-Por-CA-PEG and MSN-Por-SA-PEG and free DOX solutions in PBS were added to form culture media with different DOX concentrations (0-10.0 mg L⁻¹ DOX). The cells were subjected to MTT assay after being incubated for 24 and 48 h under light irradiation (2mW, 400-700 nm). The absorbance of the solution was measured on a Bio-Rad 680 microplate reader at 490 nm. Cell viability (%) was also calculated based on eqn (1).

3. Results and discussion

3.1 Synthesis of Zn-Por-CA-PEG

The acid sensitive PEGylated Zn-Por (Zn-Por-CA-PEG) was synthesized as the route shown in Scheme S1 and S2. Firstly, Zn-Por-CA was prepared by the ring-opening reaction between Zn-Por-NH₂ and CA, which conjugated with an amide bond. To improve the biocompatibility and stability *in vivo*, Zn-Por-CA was further PEGylated by condensation between the hydroxyl group of PEG and the carboxyl group of Zn-Por-CA. The ¹H NMR spectra shown in Fig.S1 strongly confirmed the successful synthesis of Zn-Por-CA-PEG. The peaks at -2.7 ppm (a) assigned to -NH₂ and at 4.05 ppm (b) belonged to -NH- demonstrated the successful synthesis of Por-NH₂ in Fig.S1A. Then, the peaks at -2.7 ppm disappeared after coordination between Por-NH₂ and Zinc, implying Zn-Por-NH₂ gained successfully (Fig.S1B). Shown in Fig.S1C, the disappearance of the peaks at 4.05 ppm and following the appearance of the peak at 1.5 ppm indicated the successful conjugate of Zn-Por-NH₂ and CA. Then, the peak at 3.5 ppm (d) belonged to -OCH₂CH₂O- and the peak at 11.8 ppm assigned to -COOH demonstrated the successful synthesis of Zn-Por-CA-PEG (Fig.S1D).

3.2 Synthesis of MSN-Por-CA-PEG

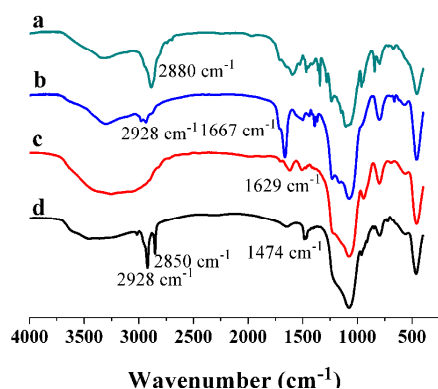


Fig. 2 FTIR spectra of MSN-Por-CA-PEG (a), MSN-His (b), MSN-NH₂ (c) and MSN-CTAB (d).

In this paper, MCM-41 type MSNs with an average diameter of 140 nm was used as a scaffold. To realize the histidine modification, MSN-NH₂ was prepared firstly. And then, Zn-Por-CA-PEG was used as a gatekeeper to block the nanopores of MSN-His by the metallo-supramolecular-coordinated interaction between Zn-Por and histidine. The FT-IR spectra of MSN-CTAB, MSN-NH₂, MSN-His and MSN-Por-CA-PEG were shown in Fig. 2. The characteristic C-H peaks at 2928, 2850 and 1474 cm⁻¹ were ascribed to a large amount of CTAB existing in the channels, implying the successful synthesis of MSN-CTAB. The disappearance of these peaks attributed to the removal of CTAB. Moreover, the peak appeared at 1629 cm⁻¹ belonged to N-H

vibration confirmed the successful synthesis of MSN-NH₂. The peaks appeared at 1667 cm⁻¹ assigned to the imine bond and at 2928 cm⁻¹ ascribed to C-H confirmed the successful modification of histidine on the surface of MSN-NH₂. The adsorption peaks at 2880 cm⁻¹, which assigned to C-H deformation vibration in PEG, indicated the successful block of Zn-Por-CA-PEG as a gatekeeper to prepare MSN-Por-CA-PEG.

According to the TGA curves of MSN-NH₂ and MSN-His (Fig. S2), the grafted ratio of His on the surface of MSN was 33 % wt, just as expected. Shown in Fig. S2, the loss weight of MSN-Zn-Por-CA-PEG is more than that of MSN-His, indicating the presence of gate keeper. According to Fig.S2, the graft ratio of His on the surface of MSN coordinated with PEG-CA-Zn-Por was 19%.

There were three diffraction peaks associated with the 100,110, and 200 reflections of hexagonal symmetry in the XRD pattern of MSN-NH₂ (Fig.3A), implying a similar ordered hexagonal mesostructure. TEM images of MSN-NH₂ particles presented uniform spherical with a mean diameter of approximately 145 nm. Besides, an array of ordered mesoporous network could be clearly observed shown in Fig.3B. After Capping, the size became bigger about 230 nm (Fig. S3). TEM of MSN-Zn-Por-CA-PEG presented similar result (Fig. S4).

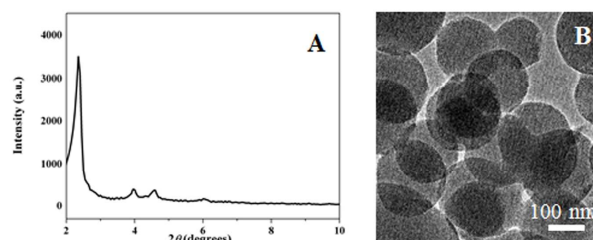


Fig. 3 Low-angle X-ray diffraction (XRD) pattern of MSN-NH₂ powders (A) and TEM image of MSN-NH₂ (B)

The surface area and pore size of MSN-NH₂ and MSN-Por-CA-PEG was examined by Brunauer-Emmett-Teller (BET) and Barrett-Joyner-Halenda (BJH) analyses. The BET surface areas of nanoparticles reduced from 1197 m²/g to 418.5 m²/g after the blocking of Por-CA-PEG to the MSN's nanopores by the metallo-supramolecular-coordination between Zn-Por-CA-PEG and histidine (Fig. 4). The BJH pore sizes of nanoparticles also reduced from 2.32 nm to 1.97 nm. These results suggest that the mesopores were successfully capped by Zn-Por-CA-PEG.

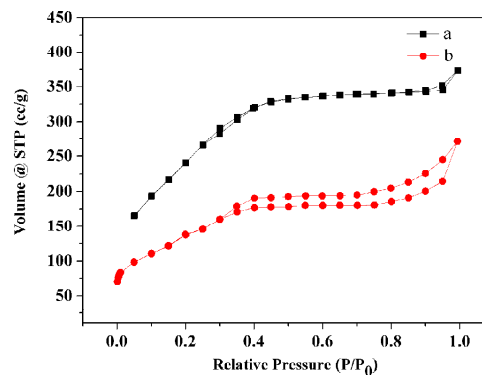


Fig. 4 Nitrogen adsorption-desorption isotherms of MSN-NH₂ (a) and MSN-Por-CA-PEG (b)

3.3 *In vitro* DOX loading and triggered release

Generally, due to high specific surface area and large pore volume, MSNs present high drug loading capacity. The DOX loading content of DOX-loaded MSN-Por-CA-PEG was calculated and as high as to be 11.2 wt%. Then *in vitro* release behaviors of DOX-loaded MSN-Por-CA-PEG were investigated at pH 5.3, 6.8 and 7.4, respectively, which were mimicking the physiological pH in late endosome, cancer extracellular microenvironment, and blood and normal tissue. About 80% of DOX was released from DOX-loaded MSNs during first 24 h in PBS at pH 5.3 shown in Fig. 5. Compared with pH 5.3, the DOX release rate accordingly reduced in pH 7.4. These different release behaviors were likely to be resulted from the acid-triggered dissociation of coordinate bond between Zn-Por and histidine, leading to the removal of the capped Zn-Por from the nanoparticle surface. Noticeably, the release ratio of DOX from DOX-loaded MSN-Por-CA-PEG was only nearly 45% and 30% at pH 6.8 and 7.4, respectively, which resulted from the blocking of gatekeeper Zn-Por-CA-PEG to the nanopores of MSN. Being blocked, drug release from the mesoporous silica more slowly than from MSN without capping (Fig. S5). So this intermediate pH-sensitive gatekeeper has the ability to enhance DOX loading content and to effectively control drug holding or rapidly release at different pH environment. Therefore, this pH-sensitive DOX-loaded MSN-Por-CA-PEG is potential as effective drug delivery system for future use.

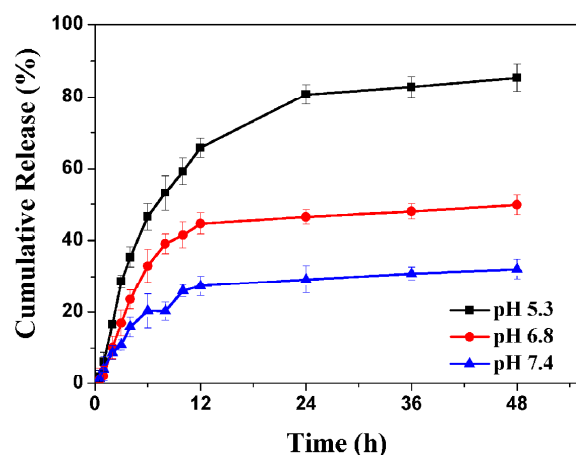


Fig. 5 *In vitro* DOX release behaviors of DOX-loaded MSN-Por-CA-PEG in PBS at pH 5.3, 6.8 and 7.4 at 37 °C

3.4 Intracellular Endocytosis

In our designed MSNs-based drug delivery system, *cis*-aconitic anhydride conjugation between Zn-Por and PEG present pH-sensitive and the amide bond formed between an amino of Zn-Por and CA is cleavable under slightly acidic condition such as pH 6.8. After cleaving of amide bond, the surface of Zn-Por becomes amino positively charged. Generally, the cell membranes are negatively charged, this positively charged MSN-Zn-Por will easily uptake by cancer cells to enhance their internalization.

To demonstrate whether MSN-Por-CA-PEG can be more efficiently internalized by cancer cells, MSN-Por-SA-PEG was synthesized as a control (Scheme S3, Fig. S6-S8). Differently, the amide bond of MSN-Por-SA-PEG is uncleavable because the linkage succinic anhydride cannot respond to pH 6.8. The ¹HNMR and FT-IR spectra demonstrated the successful synthesis of MSN-Por-SA-PEG. MSN-Por-SA-PEG also could efficiently load DOX with a drug loading content (DLC) of 11.4 wt%.

Metalloporphyrins have attracted enormous attention, not only because of its protential ability as photosensitizer but also as fluorescent probe (red). So confocal laser scanning microscopy (CLSM) and flow cytometric analyses were employed to explore the cellular uptake of MSN-Por-CA-PEG and MSN-Por-SA-PEG by HeLa cells.

After incubation with MSNs for 2 h in 37 or 4 °C, their cellular distribution was evaluated by CLSM analysis. As indicated in Fig. 6B, MSN-Por-CA-PEG was remarkably internalized at 4 °C and distributed intensively in the cytoplasm, which was rarely observed in the cells incubated with the identical MSN-Por-CA-PEG at 4 °C (Fig. 6A). Moreover, the sample incubated with MSN-Por-CA-PEG showed the strongest fluorescence intensity at 37 °C. As show in Fig. 7, the fluorescence intensity form high to low in flow cytometric analyses was in the following order: MSN-Por-CA-PEG in 37 °C (817) > MSN-Por-SA-PEG in 37 °C (346) > MSN-Por-CA-PEG in 4 °C (255) > MSN-Por-SA-PEG (186) in 4 °C, respectively (the value means the average fluorescence intensity).

These phenomena could ascribed to disconjugation of PEG and Zn-Por responded to pH 6.8, presenting positive charges and then promoting the nanoparticles enter into the cell. The results demonstrated that MSN-Por-CA-PEG could be efficiently internalized by cancer cells.

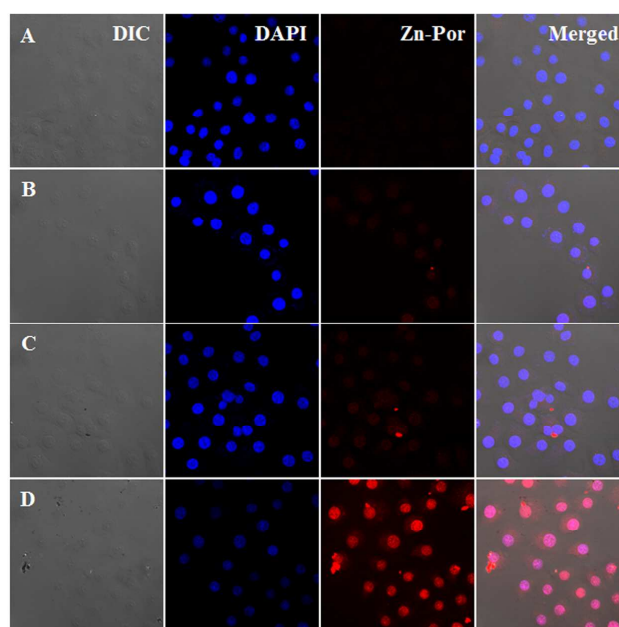


Fig. 6 Representative CLSM images of HeLa cells incubated with MSN-Por-SA-PEG (A) at 4 °C, MSN-Por-CA-PEG (B) at 4 °C, MSN-Por-SA-PEG (C) at 37 °C, and MSN-Por-CA-PEG (D) at 37 °C for 2 h. For each panel, the images from left to right show differential interference contrast (DIC) image, cell nuclei stained by DAPI (blue), Zn-Por fluorescence in cells (red), and overlays of the three images.

3.5 *In Vitro* anti-cancer efficacy

For a drug delivery, the biocompatibility is a key factor for their application. The *in vitro* cytotoxicity of MSN-Por-CA-PEG and MSN-Por-SA-PEG against HeLa and MCF-7 cells in the dark was examined by a MTT assay (Fig. S9 and S10). Free MSNs without irradiation present no obvious cytotoxicity at different concentrations, up to 10.0 g L⁻¹, indicating the excellent biocompatibility of MSNs itself as a drug carrier.

In particular, some metalloporphyrins, such as Zn-Por, have

been used as a kind of photosensitizer in clinical photodynamic therapy because of the effective generation of cytotoxic reactive oxygen species, such as singlet oxygen. However, most of porphyrins and their derivatives are hydrophobic. The lipophilic nature makes them undispersed and unstable in an aqueous medium, which greatly limits their applications *in vivo*. Taking advantage of the metallo-supramolecular-coordinated interaction, we realized not only the blocking of the nanopores of MSNs but also the co-delivery of anticancer drug and photosensitizer to enhance the water solubility and stability of them. By co-delivery and pH-controlled co-release of drug and photosensitizer “on demand”, it presents an effective way to combine chemotherapy and photodynamic therapy.

To study the anticancer efficiency of chemotherapy and PDT, we investigated thoroughly the anticancer activity *in vitro*. Firstly, singlet oxygen generated by MSNs was examined by a chemical method involving the photo-oxidation of 9,10-anthracenediyl-bis(methylene)dimalonic acid (ABDA) (Fig.S11).³⁵ The data indicated that during the light illumination in the presence of MSNs the absorption value of ABDA gradually decreased, suggesting the production of singlet oxygen. Under the same experiment condition, the amount of singlet oxygen produced by MSN-Por-CA-PEG is little more than that produced by MSN-Por-SA-PEG. To rule out the potential effect induced by light irradiation, HeLa and MCF-7 cells were irradiated directly. As shown in Fig.S12, irradiation single was no harm to cells.

Subsequently, MTT assays towards HeLa and MCF-7 cells were employed to investigate the influence of light irradiation (0.12 W/cm², 400-700 nm) on the cytotoxicity of cells *in vitro*. HeLa and MCF-7 cells were treated with a gradient concentrations of MSN-Por-CA-PEG, MSN-Por-SA-PEG, DOX-loaded MSN-Por-CA-PEG, MSN-Por-SA-PEG and free DOX under or without light irradiation for 5 min after incubation for 4 h, and then treated with MTT after 24 h. The data of cell viability were presented in Fig.8A and C. For simplicity, only the data in the case of 10.0 mg/L DOX and 9 mg/mL Zn-Por were simplified. Compared with free DOX or MSN-Por-CA-PEG with irradiation, DOX-loaded MSN-Por-CA-PEG with irradiation showed the highest cytotoxicity with the lowest cell viability, indicating the successful combination of DOX and Zn-Por, realizing synergistic chemo-photodynamic therapy to enhance the anticancer efficacy. Moreover, the cell viability of MSN-Por-CA-PEG was lower than that of MSN-Por-SA-PEG, indicating that MSN-Por-CA-PEG was easier to enter into cancer cells because the amino positively charged MSN-Zn-Por more easily enter into the negatively charged cell membranes. Furthermore, free DOX and DOX-loaded MSN without light irradiation exhibited comparable cytotoxicity, implying that single encapsulation of DOX in MSN would not obviously improve the anticancer efficacy. The cell viability towards HeLa and MCF-7 cells incubated for 48 h were also investigated, similarly, DOX-loaded MSN-Por-CA-PEG with irradiation showed the highest anticancer efficacy as shown in Fig.8B and D. Moreover, the anticancer efficacy could be improved by prolong the irradiation time. For MCF-7 cells

(Fig.8C and D), the similar results were presented, in which the lowest cell viability was 40% incubated for 24 h and 20% incubated for 48 h, respectively.

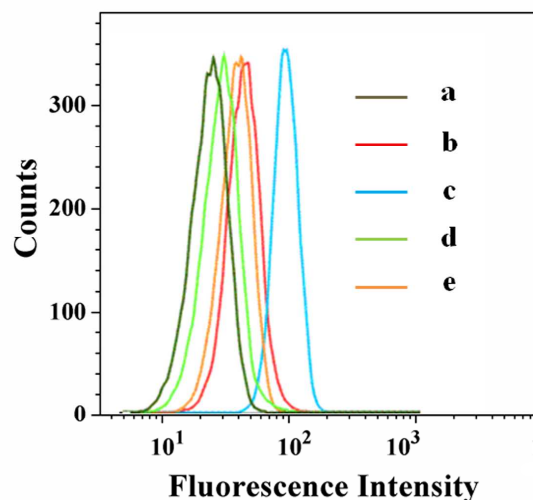


Fig. 7 Flow cytometric profiles of HeLa cells blank (a) and incubated with MSN-Por-SA-PEG (b) at 37 °C, MSN-Por-CA-PEG (c) at 37 °C, MSN-Por-SA-PEG (d) at 4 °C, and MSN-Por-CA-PEG (e) at 4 °C for 2 h

4. Conclusion

In summary, the dual pH-responsive capped MSNs was successfully prepared by the metallo-supramolecular-coordinated interaction between acid sensitive PEGylated Zn-Por and histidine, which can respond to both extracellular and intracellular pH environments to simultaneously enhance cellular uptake and promote acid-triggered intracellular drug release. Because the gatekeeper Zn-Por-CA-PEG can be used as photosensitizer in PDT, MSN-Por-CA-PEG could realize the combination of chemical therapy and PDT. The *in vitro* experiments indicated that MSNs had good biocompatibility and no toxicity towards the normal cells. Compared with the single chemotherapy of free DOX or photodynamic therapy of Zn-Por in MSNs, DOX-loaded MSN with irradiation showed higher *in vitro* anticancer therapeutic activity, potential for synergistic treatments of cancer.

Acknowledgements

This research was financially supported by the National Natural Science Foundation of China (Projects 21474012, 51273037 and 50903012), Jilin Science and Technology Bureau (20130206074GX, International Cooperation Project 20120729), Jilin Human Resources and Social Security Bureau(201125020), Jilin Environmental Protection Bureau (201127).

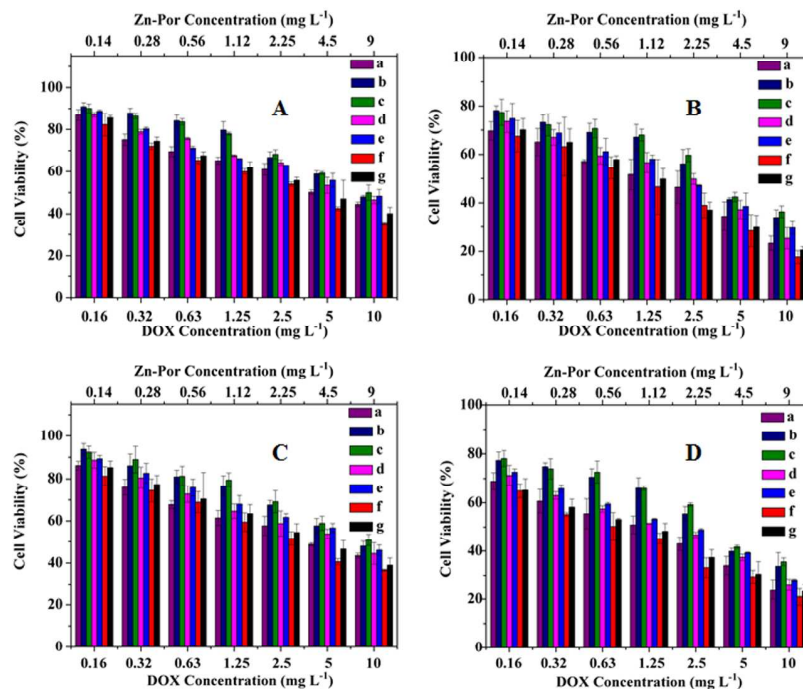


Fig. 8 Cytotoxicities of free DOX (a), MSN-Por-CA-PEG with irradiation (b), MSN-Por-SA-PEG with irradiation (c), DOX-loaded MSN-Por-CA-PEG (d), DOX-loaded MSN-Por-SA-PEG (e), DOX-loaded MSN-Por-CA-PEG with irradiation (f) and DOX-loaded MSN-Por-SA-PEG with irradiation (g) toward HeLa cells for 24 h (A), 48 h (B), and MCF-7 cells for 24 h (C), 48 h (D).

Notes and references

^aDepartment of Chemistry, Northeast Normal University, Changchun 130024, P. R. China.

*Tel.: +86 431 85099667. Fax: +86 431 85099668. E-mail: chen1686@nenu.edu.cn

^bChangchun Institute of Applied Chemistry, Chinese Academy of Sciences, Changchun 130022, P. R. China.

† Electronic Supplementary Information (ESI) available: [details of any supplementary information available should be included here]. See DOI: 10.1039/b000000x/

- N. Niu, F. He, P. Ma, S. Gai, G. Yang, F. Qu, Y. Wang, J. Xu and P. Yang, *ACS Appl. Mater. Interfaces*, 2014, **6**, 3250-3262.
- J. Croissant and J. I. Zink, *J Am Chem Soc*, 2012, **134**, 7628-7631.
- M. Frascioni, Z. Liu, J. Lei, Y. Wu, E. Strelakova, D. Malin, M. W. Ambrogio, X. Chen, Y. Y. Botros, V. L. Cryns, J. P. Sauvage and J. F. Stoddart, *J Am Chem Soc*, 2013, **135**, 11603-11613.
- S. Sahu, N. Sinha, S. K. Bhutia, M. Majhi and S. Mohapatra, *J Mater Chem B*, 2014, **2**, 3799-3808.
- M. Colilla, B. Gonzalez and M. Vallet-Regi, *Biomater. Sci.*, 2013, **1**, 114-134.
- P. Yang, S. Gai and J. Lin, *Chem Soc Rev*, 2012, **41**, 3679-3698.
- R. Hernandez, H. R. Tseng, J. W. Wong, J. F. Stoddart and J. I. Zink, *J Am Chem Soc*, 2004, **126**, 3370-3371.
- R. Liu, X. Zhao, T. Wu and P. Feng, *J Am Chem Soc*, 2008, **130**, 14418-14419.
- C. Park, K. Oh, S. C. Lee and C. Kim, *Angew. Chem. Inter. Ed.*, 2007, **46**, 1455-1457.
- X. Ji, J. Chen, X. Chi and F. Huang, *ACS Macro Letters*, 2014, **3**, 110-113.
- W. Wu, W. Driessen and X. Jiang, *J Am Chem Soc*, 2014, **136**, 3145-3155.
- E. Aznar, L. Mondragon, J. V. Ros-Lis, F. Sancenon, M. D. Marcos, R. Martinez-Manez, J. Soto, E. Perez-Paya and P. Amoros, *Angew. Chem. (Inter. in English)*, 2011, **50**, 11172-11175.
- P. D. Thornton and A. Heise, *Am Chem Soc*, 2010, **132**, 2024-2028.
- E. Secret, S. J. Kelly, K. E. Crannell and J. S. Andrew, *ACS Appl. Mater. Interfaces*, 2014, **6**, 10313-10321.
- M. Chen, X. He, K. Wang, D. He, S. Yang, P. Qiu and S. Chen, *J Mater Chem B*, 2014, **2**, 428-436.
- X. Huang and X. Du, *ACS Appl. Mater. Interfaces*, 2014, **6**, 20430-20436.
- S. Wu, Q. Deng, X. Huang and X. Du, *ACS Appl. Mater. Interfaces*, 2014, **6**, 15217-15223.
- Q. Zhao, H. Geng, Y. Wang, Y. Gao, J. Huang, Y. Wang, J. Zhang and S. Wang, *ACS Appl. Mater. Interfaces*, 2014, **6**, 20290-20299.
- Q. Yuan, Y. Zhang, T. Chen, D. Lu, Z. Zhao, X. Zhang, Z. Li, C.-H. Yan and W. Tan, *ACS Nano*, 2012, **6**, 6337-6344.
- Z. Zou, D. He, X. He, K. Wang, X. Yang, Z. Qing and Q. Zhou, *Langmuir*, 2013, **29**, 12804-12810.
- L. Xing, H. Zheng, Y. Cao and S. Che, *Adv. Mater.*, 2012, **24**, 6433-6437.
- T. Wang, L. Zhang, Z. Su, C. Wang, Y. Liao and Q. Fu, *ACS Appl. Mater. Interfaces*, 2011, **3**, 2479-2486.
- Y. Wang, K. Wang, J. Zhao, X. Liu, J. Bu, X. Yan and R. Huang, *J Am Chem Soc*, 2013, **135**, 4799-4804.
- B. C. Wilson and M. S. Patterson, *Physics in Medicine and Biology*, 2008, **53**, R61-109.

25. A. Juarranz, P. Jaen, F. Sanz-Rodriguez, J. Cuevas and S. Gonzalez, *Clinical & translational oncology : official publication of the Federation of Spanish Oncology Societies and of the National Cancer Institute of Mexico*, 2008, **10**, 148-154.
- 5 26. G. Oenbrink, P. Jurgenlimke and D. Gabel, *Photochem. and Photobio.*, 1988, **48**, 451-456.
27. U. Isele, K. Schieweck, R. Kessler, P. van Hoogevest and H. G. Capraro, *J. Pharma. Sci.*, 1995, **84**, 166-173.
28. D. Veres, B. Bocskei-Antal, I. Voszka, K. Modos, G. Csik, A. D. Kaposi, J. Fidy and L. Herenyi, *J Phys. Chem. B*, 2012, **116**, 9644-9652.
- 10 29. K. Nawalany, A. Rusin, M. Kepczynski, P. Filipczak, M. Kumorek, B. Kozik, H. Weitman, B. Ehrenberg, Z. Krawczyk and M. Nowakowska, *Inter.J Pharma.*, 2012, **430**, 129-140.
- 15 30. X. Liang, X. Li, X. Yue and Z. Dai, *Angew. Chem. Inter.Ed.*, 2011, **50**, 11622-11627.
31. D. Ma, Z. H. Liu, Q. Q. Zheng, X. Y. Zhou, Y. Zhang, Y. F. Shi, J. T. Lin and W. Xue, *Macromol. Rapid Commun.*, 2013, **34**, 548-552.
32. C. S. Lee, W. Park, Y. U. Jo and K. Na, *Chem. Commun.*, 2014, **50**, 4354-4357.
- 20 33. R. Luguya, L. Jaquinod, F. R. Fronczek, M. G. H. Vicente and K. M. Smith, *Tetrahedron*, 2004, **60**, 2757-2763.
34. X. Chen, X. Yao, Z. Zhang and L. Chen, *RSC Advances*, 2014, **4**, 49137-49143.
- 25 35. H.-L. Tu, Y.-S. Lin, H.-Y. Lin, Y. Hung, L.-W. Lo, Y.-F. Chen and C.-Y. Mou, *Adv. Mater.*, 2009, **21**, 172-177.

30

Graphical Abstract

By the metallo-supramolecular coordinated interaction between Zn-Por and histidine, a dual pH-responsive mesoporous silica nanoparticles (MSNs)-based drug delivery system has been fabricated for synergistic chemo-photodynamic therapy, which can respond to the tumor extracellular and intercellular pH stimuli.

TOC

